Dual-Sideband Receiver Enabling 160 Gbps Direct subThz-to-optical Conversion over 1400 m

Tobias Blatter[1,*], Laurenz Kulmer[1], Boris Vukovic[1], Yannik Horst[1], Marcel Destraz[2], Jasmin Smajic[1] and Juerg Leuthold[1,*]

[1]*ETH Zurich, Institute of Electromagnetic Fields, 8092 Zurich, Switzerland*
[2]*Polariton Technologies, 8134 Adliswil, Switzerland*
**Tobias.Blatter@ief.ee.ethz.ch, Juerg.Leuthold@ief.ee.ethz.ch*

Abstract: A dual-sideband reception scheme for RF links providing up to 3 dB sensitivity improvement is introduced and tested to bridge 1400 m wireless distance between 160 Gbps fiber networks at an RF of 226 GHz. © 2024 The Author(s)

1. Introduction

High-capacity wireless links with carrier frequencies above 110 GHz are considered essential for next-generation 5G and 6G mobile networks since they match the data rates of >100 Gbit/s of current fiber-optic systems [1]. Seamlessly switching between fiber-optic and wireless links is advantageous when fiber deployment is expensive or unfeasible. In contrast to optical free-space links, THz links suffer less from adverse weather conditions [2].

THz wireless links can be categorized into all-electronic, photonic-electronic, and all-photonic systems. All-electronic links use electronic mixers for signal conversion at the transmitter and the receiver [3]. All-electronic links have demonstrated line rates of 96 Gbit/s over 40 m [4], 64 Gbit/s over 850 m [5], and 10 Gbit/s over 5.8 km [6]. While electronic approaches offer high sensitivity, they are often bandwidth-limited. Therefore, even higher data rates are achieved using photonic-electronic links. These utilize photonics-based transmitters with heterodyne mixing in a uni-travelling carrier photodiode (UTC-PD). Such transmitters leverage well-established optical communication technologies, allowing for high-bandwidth transmission and integration in fiber-optic networks [3]. Recently, many photonic-electronic links have demonstrated line rates exceeding 100 Gbit/s at distances up to 110 m [7-11]. Data rates as high as 1056 Gbit/s over 3.1 m [12] have been demonstrated using polarization multiplexing and MIMO schemes. Long-range demonstrations achieved line rates of 19.6 Gbit/s over 4.6 km [13] and 50 Gbit/s over 850 m [14]. All-photonic links directly modulate the RF signal at the receiver onto an optical carrier using electro-optic modulators [15]. They offer larger bandwidths than electronic receivers and integrate seamlessly with fiber-optic networks [16]. Demonstrations achieved 30 Gbit/s over 58 m [17], 50 Gbit/s over 16 m [18], and 192 Gbit/s over 115 m [16]. However, a (sub-)THz link combining line rates above 100 Gbit/s and distances above 1 km has not yet been shown.

In this paper, we demonstrate a photonic subTHz wireless link over 1400 m, achieving a maximum achievable information rate (AIR) of 160 Gbit/s, which, to our knowledge, is the highest rate-distance product reported, see inset (I) in Fig. 1. The success is in part due to the introduction of a novel receiver scheme that captures both sidebands, yielding an SNR gain of up to 3 dB in theory and in this experiment an SNR gain of up to 2 dB.

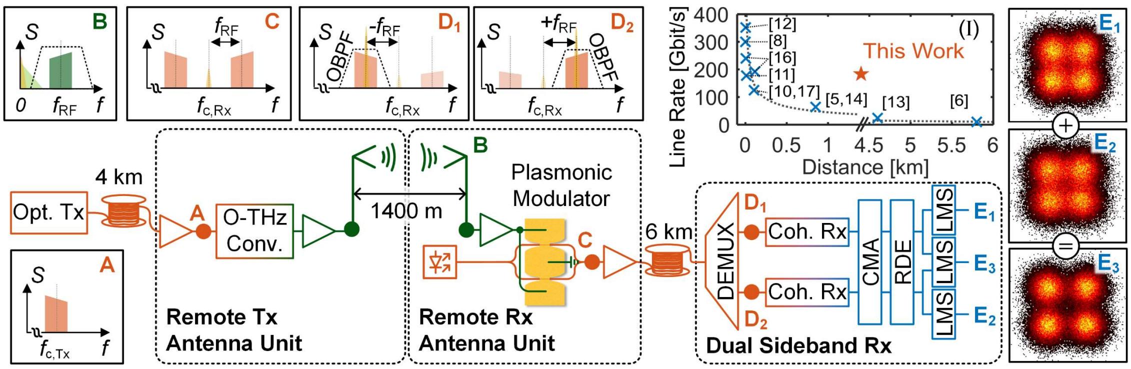

Fig. 1: Schematic of the experimental setup. It showcases the optical transmitter (Opt. Tx), optical to subTHz conversion (O-THz) utilizing heterodyne mixing in a UTC-PD. After free-space propagation of 1400 m, the THz signal directly modulates an optical signal by a plasmonic modulator. The two emerging sidebands are separately mixed to baseband using two coherent receivers mitigating the impact of the noise incurring after point C. Inset I: Line rate [Gbit/s/Pol/Ch] vs. distance of recent (sub-)THz communication links.

2. Experimental Setup

The experimental setup is illustrated in Fig. 1. The optical transmitter (Opt. Tx) utilizes a laser with a wavelength in the C-band. A Nyquist frequency division multiplexed (NFDM) and power-loaded data signal is encoded onto this laser via an IQ modulator with a 3 dB bandwidth of 38 GHz. Upon propagating through a standard single-mode fiber (SSMF) of length 4 km, emulating a remote antenna unit, and subsequent amplification, the signal is mapped onto a 226 GHz carrier. This downmixing is obtained by beating the incoming signal with a local oscillator laser in a UTC-PD. After the UTC-PD, the subTHz signal is amplified by an electrical amplifier with a gain of ~24 dB, yielding a typical output power of 12 dBm. It is then transmitted over a 1400 m free-space distance, 2 m above a predominantly meadow terrain, to the receiver. The channel loss comprises 142.5 dB of free-space path loss and 5-7 dB of atmospheric attenuation, partially compensated by two antennas having a measured combined gain of 120.7 dB. The signal after the receiving antenna is amplified by a second electrical amplifier having a gain of 24 dB and afterward fed to an organic-plasmonic MZM, where the subTHz signal is directly used to modulate the amplitude of an optical carrier at 1557.33 nm. The MZM offers a V_π of 12.3 V and a fiber-to-fiber insertion loss of 17.5 dB. At the MZM, two sidebands emerge carrying identical information and identical noise picked up to this point (C). The upper sideband (USB) and lower sideband (LSB) are separated by $2f_{\mathrm{RF}}$. After amplification by a low-noise erbium-doped amlifier (LNA), the signal propagates through a 6 km SSMF fiber before entering the dual sideband receiver. The dual sideband receiver incorporates a wavelength demultiplexer to separate the two sidebands, which are then processed by two coherent receivers (Coh. Rx), converting both sidebands to baseband. Digital signal processing subsequently combines these basebands. The dual sideband receiver makes use of the fact that both sidebands carry the same information, and the noise picked up after point C to each sideband is uncorrelated. By exploiting the information redundancy, the impact of the noise can be mitigated, resulting in an SNR gain. This noise stems predominantly from the LNA after point C. Fig. 2(a) shows the qualitative relationship between SNR after the LNA and the sideband power after the MZM (see point C). For high sideband powers, SNRs converge to the SNR at point C ($\mathrm{SNR_C}$). In this scenario, no SNR enhancement, denoted in yellow, can be realized. However, for lower received power, the amplified spontaneous emission noise from the LNA overshadows inherent transmitter noise, allowing the dual sideband Rx to achieve up to a 3 dB SNR gain compared to a single sideband reception.

3. Transmission Experiment

The transmitted signal was multiplexed into 8 NFDM channels, each with a bandwidth of 8 GHz, culminating in a total bandwidth of 64 GHz. Channels 1-8 were bit-loaded with QAM of order 8, 16, 16, 16, 4, 4, 4 and 4. Additionally, channels 1-8 were power-loaded with 1.4, -0.1, -2.9, 0.6, -2.4, -0.3, -0.8, and 2.7 dB to compensate for the frequency

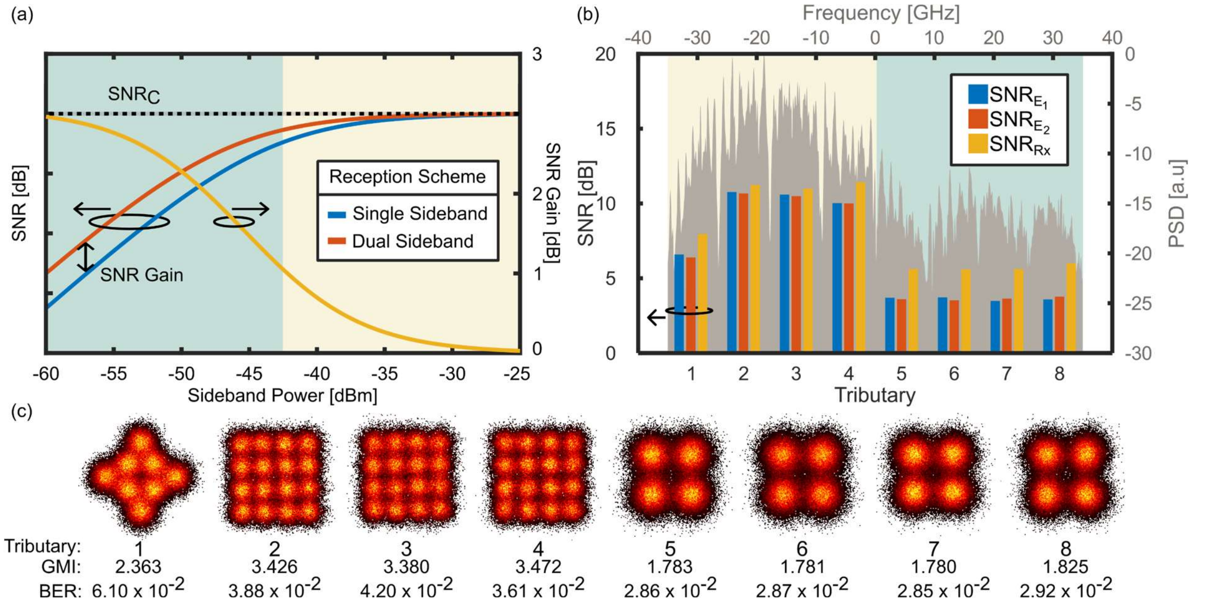

Fig. 2: (a) Left: SNR (qualitatively) after the EDFA at point C for the dual sideband (red) and single sideband (blue) receiver scheme versus sideband power at point C. Right: resulting SNR gain. (b) SNR of the single received signals (blue and red), their combination (yellow), the optical back-to-back (violet) measurement and the RF signal (green) are presented. The Rx baseband signal's power spectrum is shown in grey. (c) Constellation diagram, BER and GMI of each channel.

response of the RF components. The SNRs of the optical back-to-back (B2B) measurements of the respective NFDM channels were 17.2, 19.7, 21.3, 23.1, 21.9, 20.9, 18.6, and 16.2 dB, aggregating to a total line rate of 184 Gbit/s. The optical NFDM signal was then down-converted to a carrier frequency of 226 GHz. After amplification, the RF signal was sent to the receiver 1400 m away. At the receiver, the signal was amplified and coupled via an RF probe to the MZM, where the signal was up-converted back to the optical domain. After recording the baseband signal of the sidebands, the signals were further processed in an offline DSP. The DSP incorporated a blind constant modulus algorithm (CMA) and a blind radius-directed equalizer (RDE), followed by carrier recovery and a T/2-spaced feed-forward equalizer (FFE). The number of filter taps of the CMA, RDE, and FFE was set to 41, 41 and 223, respectively. Combining the two baseband signals was achieved by utilizing a butterfly extension of the FFE. The baseband signal spectrum is shown in Fig. 2(b). Channels 5-8 have diminished powers, attributable to the reduced output power of the UTC-PD and electrical amplifiers at these frequencies. The spectrum also reveals ripples that we attribute to resonances in the RF part.

4. Results and Discussion

The new receiver scheme yielded an SNR gain of up to 2 dB, boosting the net data rate by over 10% to a total maximum AIR of 160 Gbit/s. The AIR was calculated by the product of the average general mutual information (GMI) of all tributaries and the total symbol rate of 64 GBaud. The constellation diagram, the bit-error rate, and GMI of each tributary are presented in Fig. 2(c). In detail, the single-received LSB signal's average GMI was 2.25 bit/symbol, corresponding to an AIR of 144.0 Gbit/s. When combined with the USB signal in the dual sideband reception scheme, the net information rate increased to 2.48 bit/symbol, resulting in an AIR of 158.7 Gbit/s.

In Fig. 2(b), we show the measured $\mathrm{SNR}_{\mathrm{E}_1}$ in blue and $\mathrm{SNR}_{\mathrm{E}_2}$ in red of the NFDM tributaries at the receiver. We also show the combined SNR ($\mathrm{SNR}_{\mathrm{R_x}}$) in yellow. We can report an SNR gain of up to 2 dB for the tributaries with poor SNRs. The fact that the received signals from tributaries 5 to 8 have low powers shows that the THz transmitter in this frequency range does not provide sufficient output power. This results in low SNR values. Yet, these tributaries experience the largest SNR gain and benefit, therefore, the most from the dual reception scheme.

In summary, we demonstrated an all-photonic optical-subTHz-optical link, achieving an AIR of 160 Gbit/s over 1400 m free-space distance. To the best of our knowledge, this results in a record rate-distance product of 224 Gbit/s·km. This was enabled by the use of the dual-sideband reception scheme, which yielded an enhancement in SNR of up to 2 dB.

5. Acknowledgements

We thank Innovation Park Zurich, ArmaSuisse, Dübendorf Airport, the H2020 projects VERTIGO (822030) and PlasmoniAC (871391), and Polariton Technologies for providing the plasmonic MZM. Polariton thanks NLM Photonics for the organic EO material.

6. References

[1] Y. Li *et al.*, "Fixed Wireless Communication Links Beyond 100 GHZ," in *APMC*, 2018, pp. 31-33.
[2] T. S. Rappaport *et al.*, "Wireless Communications and Applications Above 100 GHz: Opportunities and Challenges for 6G and Beyond", IEEE Access, 2019, vol. 7, pp. 78729-78757.
[3] T. Nagatsuma *et al.*, "Advances in terahertz communications accelerated by photonics", Nat Photonics, 2016, vol. 10, no. 6, pp. 371-379.
[4] F. Boes *et al.*, "Ultra-broadband MMIC-based wireless link at 240 GHz enabled by 64GS/s DAC," in *IRMMW-THz*, 2014, pp. 1-2.
[5] I. Kallfass *et al.*, "64 Gbit/s Transmission over 850 m Fixed Wireless Link at 240 GHz Carrier Frequency", J. Infrared Millim. Terahertz Waves, 2015, vol. 36, no. 2, pp. 221-233.
[6] A. Hirata *et al.*, "5.8-km 10-Gbps data transmission over a 120-GHz-band wireless link," presented at the ICWITS, 2010.
[7] S. Koenig *et al.*, "Wireless sub-THz communication system with high data rate", Nat Photonics, 2013, vol. 7, no. 12, pp. 977-981.
[8] X. Pang *et al.*, "260 Gbit/s photonic-wireless link in the THz band," presented at the IPC, 2016.
[9] T. Harter *et al.*, "Generalized Kramers-Kronig receiver for coherent terahertz communications", Nat Photonics, 2020, vol. 14, no. 10, pp. 601.
[10] J. Ding *et al.*, "104-m Terahertz-Wave Wireless Transmission Employing 124.8-Gbit/s PS-256QAM Signal," presented at the OFC, 2022.
[11] S. Jia *et al.*, "Integrated dual-laser photonic chip for high-purity carrier generation enabling ultrafast terahertz wireless communications", Nat. Commun., 2022, vol. 13, no. 1, pp. 1388.
[12] X. Li *et al.*, "1-Tb/s Millimeter-Wave Signal Wireless Delivery at D-Band", 2019, vol. 37, no. 1, pp. 196-204.
[13] W. Li *et al.*, "Photonics-Aided THz-Wireless Transmission over 4.6 km Free Space by Plano-Convex Lenses," in *ECOC*, 2022, pp. 1-4.
[14] W. Li *et al.*, "Photonics-assisted 320 GHz THz-band 50 Gbit/s Signal Outdoor Wireless Communication over 850 Meters," presented at the Optical Fiber Communications Conference and Exhibition (OFC), 2023.
[15] Y. Salamin *et al.*, "Microwave plasmonic mixer in a transparent fibre–wireless link", 2018, vol. 12, no. 12, pp. 749-753.
[16] Y. Horst *et al.*, "Transparent Optical-THz-Optical Link at 240/192 Gbit/s Over 5/115 m Enabled by Plasmonics", J Lightwave Technol, 2022, vol. 40, no. 6, pp. 1690-1697.
[17] T. Harter *et al.*, "Wireless THz link with optoelectronic transmitter and receiver", Optica, 2019, vol. 6, no. 8, pp. 1063-1070.
[18] S. Ummethala *et al.*, "THz-to-optical conversion in wireless communications using an ultra-broadband plasmonic modulator", Nat. Photonics, 2019, vol. 13, no. 8, pp. 519.